EUROPHYSICS LETTERS

OFFPRINT

Vol. 65 • Number 5 • pp. 587–593

Quantized AC-Stark shifts and their use for multiparticle entanglement and quantum gates

* * *

F. Schmidt-Kaler, H. Häffner, S. Gulde, M. Riebe, G. Lancaster, J. Eschner, C. Becher and R. Blatt

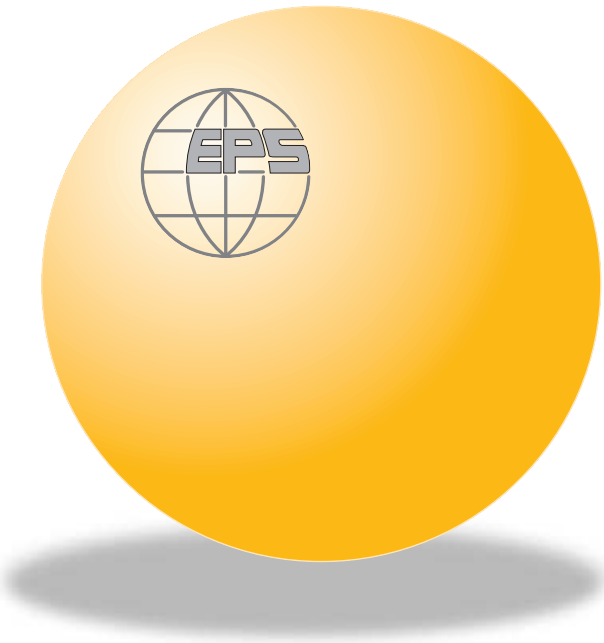

Published under the scientific responsibility of the

EUROPEAN PHYSICAL SOCIETY

Incorporating

JOURNAL DE PHYSIQUE LETTRES • LETTERE AL NUOVO CIMENTO

EUROPHYSICS LETTERS 1 March 2004

Europhys. Lett., **65** (5), pp. 587–593 (2004)
DOI: 10.1209/epl/i2003-10174-3

Quantized AC-Stark shifts and their use for multiparticle entanglement and quantum gates

F. Schmidt-Kaler, H. Häffner, S. Gulde, M. Riebe, G. Lancaster, J. Eschner, C. Becher and R. Blatt

Institut für Experimentalphysik - 6020 Innsbruck, Austria

(received 5 September 2003; accepted 18 December 2003)

PACS. 03.67.Lx – Quantum computation.
PACS. 03.65.Ud – Entanglement and quantum nonlocality (*e.g.*, EPR paradox, Bell's inequalities, GHZ states, etc.).

Abstract. – A single $^{40}Ca^{+}$-ion is trapped and laser-cooled to its motional ground state. Laser radiation which couples off-resonantly to a motional sideband of the ion's $S_{1/2}$ to $D_{5/2}$ transition causes a phase shift proportional to the ion's motional quantum state $|n\rangle$. As the phase shift is conditional upon the ion's motion, we are able to demonstrate a universal 2-qubit quantum gate operation where the electronic target state $\{S, D\}$ is flipped depending on the motional qubit state $|n\rangle = \{|0\rangle, |1\rangle\}$. Finally, we discuss scaling properties of this universal quantum gate for linear ion crystals and present numerical simulations for the generation of a maximally entangled state of five ions.

Trapped ions are successfully used for quantum information processing [1–3] as experiments with a single-ion [4–7] and two-ion crystals [8,9] have proven. Even four-ion crystals [10] have been transferred into an entangled state. Since entanglement distinguishes quantum mechanics from wave mechanics, its investigation helps to understand the borderline between quantum and classical physics. Therefore, it is of fundamental importance to create states of many entangled particles. On the other hand, in quantum information processing two-qubit gate operations can be used to create entangled states. For most implementations of these gate operations, a well-defined phase shift (a phase gate) is induced, depending on the qubit's quantum states. Its origin might be either a geometric phase [11,12] as the quantum state follows a closed loop in phase space [8], or the sign of the wave function is changed as a resonant 2π-Rabi rotation is performed [4, 9, 13]. Alternatively, the phase shift which is required for the gate operation may be derived from a non-resonant laser-atom interaction [14]. The resulting quantum phase gate Φ transforms the state of two qubits $|a, b\rangle \rightarrow \exp[i\phi\delta_{1,a}\delta_{1,b}]|a, b\rangle$, where $\delta_{1,a}$ and $\delta_{1,b}$ denote Kronecker symbols with $\delta_{1,a} = 1$ if qubit a is in the state $|1\rangle$ and $\delta_{1,a} = 0$ otherwise. Only for both qubits in $|1\rangle$, the quantum state's phase is shifted by ϕ. This phase gate may be converted into a controlled-NOT operation (CNOT) by single qubit rotations before and after performing Φ to yield $|a, b\rangle \rightarrow |a, a \oplus b\rangle$, where $\oplus$ represents an addition modulo 2.

A quantum phase gate [15] also has been demonstrated using long-lived superpositions of Rydberg atoms which traverse a high-Q microwave cavity. The phase ϕ of a superposition $(|0\rangle + e^{i\phi}|1\rangle)/\sqrt{2}$, where $|0\rangle$ and $|1\rangle$ denote the qubit states, is changed conditioned on the quantum state of the cavity mode. If the cavity resonance is detuned slightly from that of the atomic qubit transition, superpositions acquire a significant light shift already by a single photon stored in the microwave cavity [16].

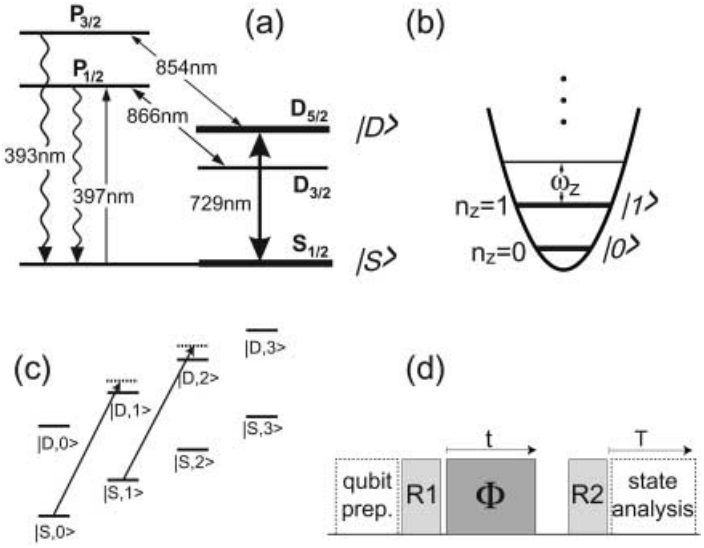

Fig. 1 – a) $^{40}Ca^{+}$ level scheme. A qubit is encoded in the $S_{1/2}, (m = -1/2)$ ground and $D_{5/2}, (m = -1/2)$ metastable state. b) The lowest two number states n of the axial vibrational motion in the trap form the other qubit. c) Non-resonant interaction with the laser tuned close to the upper motional sideband (indicated by arrows). d) Laser pulse sequence for the quantum gate, consisting of the preparation of qubit states, single-bit operations $R1$ and $R2$ and controlled phase shift operation Φ of duration t. Finally, the qubits are analyzed for their electronic and motional quantum state.

In this paper we study experimentally and theoretically the dispersive (off-resonant) coupling of laser radiation for quantum information processing with trapped ions. The quantum information is encoded in the ion's electronic ground state $S_{1/2}, (m = -1/2) \equiv |S\rangle$ and a long-lived metastable state $D_{5/2}, (m = -1/2) \equiv |D\rangle$ (see fig. 1a). The qubit can be manipulated by laser radiation near 729 nm on the corresponding quadrupole transition. In the first part of the paper, we describe how to induce and to determine a phase shift of a single qubit in the superposition $|S + D\rangle/\sqrt{2}$ depending on the Fock state in which the motional state is prepared (see fig. 1a). We verify that this quantized AC-Stark shift is proportional to the vibrational quantum number n of the Fock state by preparing the ion in $n = 0, 1, 2, 3$. Adding single qubit rotations on the $|S\rangle$-$|D\rangle$-manifold, we implement a CNOT operation where the motional qubit ($n = 0, 1$) serves as the controlling qubit and the ions electronic states ($|S\rangle$, $|D\rangle$) represent the target qubit. Finally, we generalize this procedure to strings of ions and we show theoretically that the use of quantized AC-Stark shift is well suited to create entanglement between many ions.

In our experiment, a single $^{40}Ca^{+}$ ion is stored in a linear Paul trap with a radial and axial frequency of $\omega_{\rm rad}/2\pi = 4.9\,\text{MHz}$ and $\omega_{\rm ax}/2\pi = 1.712\,\text{MHz}$, respectively. Doppler cooling, followed by sideband ground-state cooling and optical pumping leads to a population of the state $S_{1/2}, (m = -1/2) \equiv |S\rangle$ and its lowest motional quantum state $|n = 0\rangle$ with more than 98% probability. The internal state is detected by electron shelving [5] with an efficiency $> 99\%$. We determine the occupation probability of the $|D\rangle$ state, P_D, by averaging over 100 experimental sequences. Details of the cooling method and the experimental apparatus are described elsewhere [5,17]. Starting from the state $|S, n = 0\rangle$, laser pulses resonant to the blue axial sideband ($|S, n\rangle \leftrightarrow |D, n + 1\rangle$) and resonant to the carrier transition ($|S, n\rangle \leftrightarrow |D, n\rangle$) of the qubit transition are used to transfer the motional state to Fock states [5]. The transfer

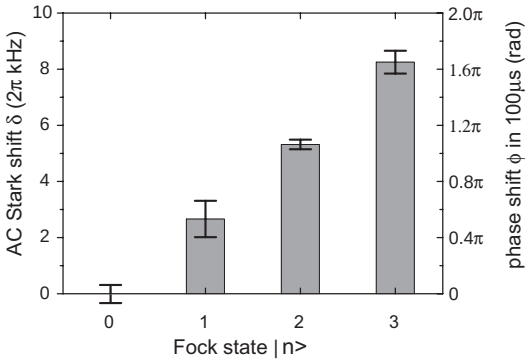

Fig. 2 – Residual AC-Stark shift (left axis) and the corresponding phase shift of the wave function (right axis) for states with up to $n = 3$ axial phonons. A linear fit yields $\delta_{\rm res}/2\pi = 2.71(6)\,$kHz per phonon. Here, the phase-shifting laser is detuned from the blue axial sideband by $\Delta = 60\,$kHz.

quality of blue sideband π-pulse and carrier π-pulse exceed 98% and 99%, respectively. Thus, we yield the desired motional Fock state with $n = 1$, 2 and 3 with fidelities better than 96%, 94% and 92%, respectively.

The phase evolution of the atomic wave function due to interaction with non-resonant laser radiation is probed in a Ramsey experiment: A resonant $\pi/2$ pulse ($R1$ in fig. 1d) on the quadrupole transition prepares the electronic qubit in the superposition state $(|S\rangle + |D\rangle)/\sqrt{2}$. A second resonant $\pi/2$ laser pulse, $R2$, is applied with opposite laser phase and a delay of $t = 260\,\mu$s. If the atomic wave function does not acquire any additional phase during the delay time, $R2$ would undo the operation of $R1$ and transfer the electronic state back to $|S\rangle$.

For the generation of a deterministic phase shift during the delay time, the ion is exposed to laser light which is blue-detuned by Δ from the blue axial sideband of the qubit transition. The resulting phase (AC-Stark) shift is due to i) off-resonant coupling to dipole transitions (see fig. 1a), ii) off-resonant coupling to carrier transitions of the $S_{1/2}$ to $D_{5/2}$ Zeeman manifold and iii) off-resonant coupling to the motional sidebands of the qubit transition. An extensive study of the first two contributions is given in [17].

The relative strengths of the three contributions scale with their respective Rabi frequencies. Thus, the light (AC-Stark) shift $\delta_{\rm iii)} = \Omega^2_{n,n+1}/4\Delta$ due to the third contribution is weaker by almost two orders of magnitude compared with i) and ii), as the resonant Rabi frequency of the blue sideband between $|S, n\rangle$ and $|D, n+1\rangle$ is given by

$$\Omega_{n,n+1} = \eta\Omega_0\sqrt{n+1} \tag{1}$$

with the Lamb-Dicke factor $\eta = 0.068 \ll 1$. As $\delta_{\rm iii)}$ strongly depends on the motional quantum number it can be utilized to generate conditional phase shifts. However, the stronger contributions i) and ii) mask this effect. Therefore we cancel i) and ii) using an additional off-resonant light field with equal, but opposite phase shift ("compensating" light field) which illuminates the ions during the phase shift operation [17]. This light field is derived from the same laser source near 729 nm which we use for the qubit transition using an acousto-optical modulator. By optimizing the compensation light field parameters, *i.e.* laser intensity and detuning, we also cancel the light shift for the motional Fock state $|n = 0\rangle$. For this state the compensation leads to a residual light shift of $\delta/2\pi \leq 300\,$Hz (see fig. 2). Thus, after compensation, the phase shift $\Delta\phi = \delta_{\rm iii)}t$ is directly proportional to the motional quantum

number n of the ion,

$$\Delta\phi = \frac{\eta^2\Omega_0^2 t}{4\Delta} n, \tag{2}$$

where t denotes the duration of the phase shift operation in the sequence. For the Fock states $|n=1\rangle$ to $|n=3\rangle$, we observe a linear slope of $\delta_{\mathrm{iii})}/2\pi = 2.71(6)\,\mathrm{kHz}$ per phonon (see fig. 2).

In order to realize a phase gate operation, we chose $t = t_0$ such that the residual phase shift for states with $n = 1$ yields precisely $\pi/2$. This accomplishes a quantum gate in the two-qubit computational space composed by the states $|S,0\rangle$, $|D,0\rangle$, $|S,1\rangle$ and $|D,1\rangle$: the states $|S,1\rangle$ and $|D,1\rangle$ acquire phases of $e^{\pm i\pi/2} = \pm i$, respectively, while $|S,0\rangle$ and $|D,0\rangle$ do not acquire any phase. Thus the phase shift operation Φ reads:

$$\Phi(t_0) = \begin{pmatrix} 1 & 0 & 0 & 0 \\ 0 & 1 & 0 & 0 \\ 0 & 0 & i & 0 \\ 0 & 0 & 0 & -i \end{pmatrix}.$$

The Ramsey pulses $R1$ and $R2$ are represented by

$$\frac{1}{\sqrt{2}} \begin{pmatrix} 1 & \pm i & 0 & 0 \\ \pm i & 1 & 0 & 0 \\ 0 & 0 & 1 & \pm i \\ 0 & 0 & \pm i & 1 \end{pmatrix},$$

where the $+$ $(-)$ sign refers to $R1(R2)$. The full sequence C represents a universal two-qubit gate:

$$C = R2\Phi(t_0)R1 = \begin{pmatrix} 1 & 0 & 0 & 0 \\ 0 & 1 & 0 & 0 \\ 0 & 0 & 0 & -1 \\ 0 & 0 & 1 & 0 \end{pmatrix}.$$

In the experiment, the truth table of this gate is probed by preparing the four computational basis input states. After the gate operation C, the internal state $\{S, D\}$ which served as the target qubit is detected by electron shelving. For detection of the motional state $n = \{0, 1\}$, *i.e.* the control qubit, we drive Rabi oscillations on the blue axial sideband. These Rabi oscillations are plotted in fig. 3. In a first step, we determine the Rabi frequencies by fitting the data with pure sine-functions. From this fit we determine $\Omega_{0,1}/2\pi = 11.9\,\mathrm{kHz}$ and $\Omega_{1,2}/2\pi = \sqrt{2}\Omega_{0,1}$ (cf. fig. 3). In a next step, we fit the respective experimental data in fig. 3a-d with a model function:

$$P_D(\tau) \;=\; a_{S0}\sin^2(\Omega_{0,1}\tau) + a_{D0} + a_{S1}\sin^2(\Omega_{1,2}\tau) + a_{D1}\cos^2(\Omega_{0,1}\tau). \tag{3}$$

The coefficients a_{S0}, a_{D0}, a_{S1}, a_{D0} account for the contributions of the four computational basis states $|S,0\rangle, |D,0\rangle$, $|S,1\rangle$, $|D,1\rangle$ and obey $a_{S0} + a_{D0} + a_{S1} + a_{D1} = 1$. The table in fig. 4 lists these coefficients for the four different input states. We find transfer efficiencies between the ground state $|S,0\rangle$ and the desired output states of $\geq 81\%$. The measured efficiencies are attributed to the following experimentally determined imperfections: i) state preparation as mentioned above (ground-state cooling and preparation pulses); ii) the chosen gate interaction time $t_0 = 200\,\mu\mathrm{s}$ which has been off by $+$ 8% from its ideal value; iii) the independently measured loss of coherence ($\simeq 6\%$) of the qubit [18] within the delay time between $R1$ and $R2$; and iv) off-resonant sideband and carrier excitations during Φ [19], measured here to account for an error of 4%.

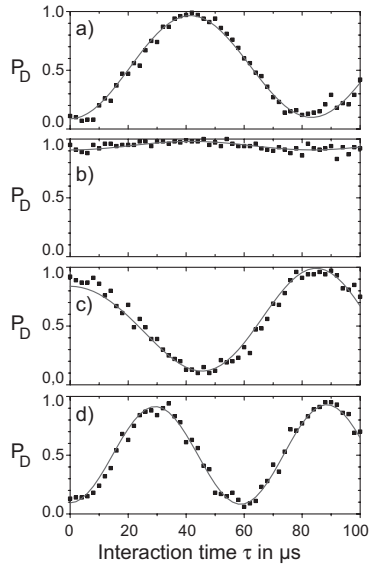

Fig. 3 – State analysis after the gate operation for input states $|S,0\rangle$ (a), $|D,0\rangle$ (b), $|S,1\rangle$ (c) and $|D,1\rangle$ (d). The ion interacts on the blue sideband ($|S,n\rangle \leftrightarrow |D,n+1\rangle$) resonant for a time τ. A fit of pure sine-functions yields Rabi frequencies of $\Omega_{0,1}/2\pi = 11.9(1)\,\mathrm{kHz}$ (a), $12.0(2)\,\mathrm{kHz}$ (c) and $\Omega_{1,2}/2\pi = 16.95(5)\,\mathrm{kHz}$ (d). The frequency ratios of (d) and (a), $\sqrt{2.02(4)}$, and of (d) and (c), $\sqrt{1.99(7)}$ agree well with the expected factor $\sqrt{2}$ from eq. (1). The solid lines correspond to a fit of the model function eq. (3).

The demonstrated dispersive two-qubit gate can be extended to a larger number of N qubits. An important advantage of dispersive gates, like, *e.g.*, the gate presented in ref. [8], is that the computational subspace is conserved automatically as the off-resonant interaction Φ only modifies the phase. Other gate schemes need auxiliary levels [4, 13] or composite pulse techniques [7] thus increasing the technical complexity of the experimental sequence.

For the entangling operation, we select a symmetric vibrational mode (bus mode) where each ion has the same oscillation amplitude (*i.e.* the absolute values of the ions' Lamb-Dicke

input	S, 0	D, 0	S, 1	D, 1
S, 0	**0.90(1)**	0.06(1)	0.01(2)	0.03(1)
D, 0	0.09(1)	**0.89(1)**	0.00(1)	0.02(1)
S, 1	0.00(1)	0.03(1)	0.16(2)	**0.81(2)**
D, 1	0.07(1)	0.00(1)	**0.84(2)**	0.09(2)

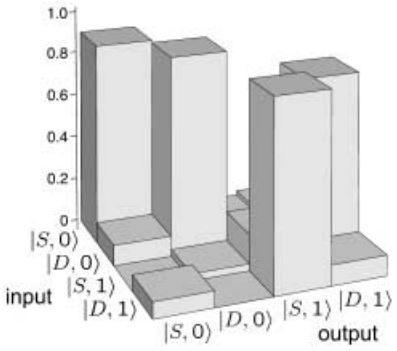

Fig. 4 – Experimentally obtained truth table of the gate including the imperfect input state preparation.

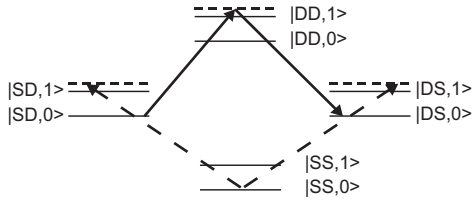

Fig. 5 – Level scheme of a two-ion crystal up to phonon number of $n = 1$. The virtual levels detuned from the blue sideband are indicated as dashed horizontal lines. The solid arrows represent the Raman-like coupling between $|SD, 0\rangle$ and $|DS, 0\rangle$. The dashed arrows symbolize the off-resonant phase changing coupling of the $|SS, 0\rangle$ levels on the blue sideband.

parameters are equal), *e.g.* the center-of-mass mode. This is crucial for the scheme to work, since otherwise each ion would have a different coupling strength to the laser field. Similar to the one-ion gate operation, the N-ion string is assumed to be cooled close to the motional ground state (*e.g.*, by EIT-cooling [20]). To create an entangled state, we use a pulse sequence $R2\Phi(t_0)R1$ acting in the following way: $R2\Phi(t_0)R1|SS\ldots S\rangle = |SS\ldots S\rangle + \mathrm{e}^{i\phi}|DD\ldots D\rangle$. First, we consider the two-ion case. The two ions are excited by a $R1$ pulse as defined above yielding the superposition state $1/2(|SS\rangle + |SD\rangle + |DS\rangle + |DD\rangle)$. The phase operation $\Phi(t_0)$ then couples the ions via the bus mode. The phase of the final $\pi/2$ Ramsey pulse $R2$ has to be chosen $\pi(\pi/2)$ relative to $R1$ for an odd (even) number of ions. Note that this scheme only requires the same Rabi frequency for all ions, but no individual addressing of the ions. This can be conveniently achieved by illuminating the ions along the trap axis. The crucial part of the operation is contained in $\Phi(t_0)$: The fraction of the superposition being in the $|DD\rangle$ state remains completely unchanged, since the phase shift induced by the laser is cancelled by the compensation laser (see [17]). Similary to the one-ion case, the $|SS\rangle$ part, however, acquires a phase factor without a change in population. Choosing the pulse length t_0, Rabi frequency Ω and detuning Δ of the sideband interaction such that $t_0 = \Delta/(\eta^2\Omega^2)$, the acquired phase factor of the $|SS\rangle$ state is -1. For ions where both qubit levels are populated, Raman processes take place (see fig. 5) where the populations of the $|SD\rangle$ and $|DS\rangle$ are exchanged and additionally a phase factor of -1 is acquired for both states. The entangling mechanism is reminiscent of the Mølmer-Sørensen scheme which, however, uses a non-resonant bichromatic light field [21].

A similar reasoning holds for N ions as verified by numerical simulations. Taking $N = 5$ as example, we chose the parameters $\Omega = 2\pi \times 230\,\mathrm{kHz}$, $\Delta = 2\pi \times 60\,\mathrm{kHz}$, and $\eta = 0.068/\sqrt{5}$. In addition to the bus mode (center of mass), the two closest spectator modes were taken into account. After an interaction time of $900\,\mu\mathrm{s}$ a state

$$|\Psi\rangle \;=\; \sqrt{0.48}|SSSSS, 000\rangle + \mathrm{e}^{i\phi}\sqrt{0.45}|DDDDD, 000\rangle + \sqrt{0.07}|\epsilon\rangle \tag{4}$$

is achieved, where $|\ldots, n_b n_{s_1} n_{s_2}\rangle$ refers to the phonon numbers of the bus mode and two of the spectator modes, respectively. $|\epsilon\rangle$ is a superposition of all undesired states with mostly zero phonon excitation. The population in $|\epsilon\rangle$ could be reduced further by reducing the gate speed. The simulations take into account most of our current experimental parameters and imperfection. The scheme does not require ground-state cooling of the bus mode. However, since each ion in the string has a different Lamb-Dicke factor for the spectator modes, the coupling of these modes to the laser should be reduced as much as possible. Otherwise, the laser-ion coupling would be slightly different for the different ions resulting in less precise Raman-π-pulses. Therefore, cooling of the spectator modes near ground state is helpful.

A spin-echo technique reduces the influence of frequency fluctuations which are slow compared to the entangling time. Applying this technique, we expect an interference contrast of more than 0.9 over 2 ms with a single ion. Thus, we find that —for our current experimental imperfections— it is reasonable to entangle 5 ions with fidelities of about 80%. Unlike most other proposals the entangling time is $\sim \sqrt{N}$ and works for any number of ions.

In conclusion, we have demonstrated a dispersive quantum gate operation employing light shifts conditional on the vibrational quantum number in a single ion. With numerical simulations, we explore the scheme for larger ion numbers and propose the generation of maximally entangled states for ion crystals with high fidelities.

REFERENCES

[1] Bouwmeester D., Ekert A. and Zeilinger A. (Editors), *The Physics of Quantum Information* (Springer, Berlin) 2000.

[2] Nielsen M. A. and Chuang I. L., *Quantum Computation and Quantum Information* (Cambridge University Press, Cambridge) 2000.

[3] A Quantum Information Science and Technology Roadmapping Project by the Advanced Research and Development Activity (ARDA), `http://qist.lanl.gov/`.

[4] Monroe C., Meekhof D. M., King B. E., Itano W. M. and Wineland D. J., *Phys. Rev. Lett.*, **75** (1995) 4714.

[5] Roos Ch., Zeiger Th., Rohde H., Nägerl H. C., Eschner J., Leibfried D., Schmidt-Kaler F. and Blatt R., *Phys. Rev. Lett.*, **83** (1999) 4713.

[6] DeMarco B., Ben-Kish A., Leibfried D., Meyer V., Rowe M., Jelenkovi B. M., Itano W. M., Britton J., Langer C., Rosenband T. and Wineland D. J., *Phys. Rev. Lett.*, **89** (2003) 267901.

[7] Gulde S., Riebe M., Lancaster G. P. T., Deuschle T., Becher C., Eschner J., Häffner H., Schmidt-Kaler F. and Blatt R., *Nature*, **422** (2003) 48.

[8] Leibfried D., DeMarco B., Meyer V., Lucas D., Barrett M., Britton J., Itano W. M., Jelenkovic B., Langer C., Rosenband T. and Wineland D. J., *Nature*, **422** (2003) 412.

[9] Schmidt-Kaler F., Häffner H., Riebe M., Gulde S., Lancaster G. P. T., Deuschle T., Becher C., Roos C. F., Eschner J. and Blatt R., *Nature*, **422** (2003) 408.

[10] Sackett C. A., Kielpinski D., King B. E., Langer C., Meyer V., Myatt C. J., Rowe M., Turchette Q. A., Itano W. M., Wineland D. J. and Monroe C., *Nature*, **404** (2000) 256.

[11] Sjöqvist E., Pati A. K., Ekert A., Anandan J. S., Ericsson M., Oi D. K. L. and Vedral V., *Phys. Rev. Lett.*, **85** (2000) 2845.

[12] Duan L. M., Cirac J. I. and Zoller P., *Science*, **292** (2001) 1695.

[13] Cirac J. I. and Zoller P., *Phys. Rev. Lett.*, **74** (1995) 4091.

[14] Solano E., arXiv:quant-ph/0310007.

[15] Rauschenbeutel A., Nogues G., Osnaghi S., Bertet P., Brune M., Raimond J. M. and Haroche S., *Phys. Rev. Lett.*, **83** (1999) 5166.

[16] Brune M., Nussenzveig P., Schmidt-Kaler F., Bernardot F., Maali A., Raimond J. M. and Haroche S., *Phys. Rev. Lett.*, **72** (1994) 3339.

[17] Häffner H., Gulde S., Riebe M., Lancaster G., Becher C., Eschner J., Schmidt-Kaler F. and Blatt R., *Phys. Rev. Lett.*, **90** (2003) 143602.

[18] Schmidt-Kaler F., Gulde S., Riebe M., Deuschle T., Kreuter A., Lancaster G. P. T., Becher C., Eschner J., Häffner H. and Blatt R., *J. Phys. B*, **36** (2003) 623.

[19] Steane A., Roos C. F., Stevens D., Mundt A., Leibfried D., Schmidt-Kaler F. and Blatt R., *Phys. Rev. A*, **62** (2000) 042305.

[20] Schmidt-Kaler F., Eschner J., Morigi G., Roos C. F., Leibfried D., Mundt A. and Blatt R., *Appl. Phys. B*, **73** (2001) 807.

[21] Sørensen A. and Mølmer K., *Phys. Rev. Lett.*, **82** (1999) 1971.